Single-unit activity evoked by electrical stimulation of human epileptogenic cortex

#606.08

Andrei Barborica[1,2], Cristian Donos[1], Ioana Mindruta[3], Jean Ciurea[4]

[1]Physics Department, University of Bucharest, Bucharest, Romania; [2]FHC Europe, Bucharest, Romania ; [3]Neurology, University Emergency Hospital, Bucharest, Romania ; [4]Neurosurgery, Bagdasar-Arseni Emergency Hospital, Bucharest, Romania

Objectives

Intracranial direct electrical stimulation (DES) during presurgical stereoelectroencephalograpic (SEEG) evaluation of patients with drug-resistent epilepsy is a powerful method for mapping the epileptogenicity of various brain areas.

In order to elucidate the basic neural mechanisms underlying electrographic responses to DES, our main objective is to investigate human single unit firing during intraoperative DES of epileptogenic areas for different stimulation amplitudes and frequencies.

The specific aims of this study are:

1. Compare the single-unit activity of neurons in epileptogenic and normal cortical areas.
2. Evaluate the effect of the frequency of the stimulation pulses on the firing patterns and rates.
3. Evaluate the time course of the firing rate during stimulation. Activity changes during stimulation have been shown to be associated with increased plasticity in the epileptogenic areas (David et al ., 2007)
4. Evaluate the entrainment of the neuronal activity by the stimulation pulses.
5. Correlate biomarkers of the epileptogenic zone identified in the EEG responses evoked by single-pulse stimulation with the single-unit firing patterns. These include delayed responses (Valentin et al, 2002), high-frequency oscillations (van't Klooster 2010).

Methods

We performed SEEG presurgical evaluation of 11 patients with drug-resistant focal epilepsy to locate the seizure-onset zone (SOZ) and delineate the area to be resected.

Patient	Sex	Age	Pathology	Epilepsy	SOZ
1	F	32	Type I cortical dysplasia	Temporal	Mesial structures
2	M	46	Hippocampal sclerosis	Mesio-temporal	Amygdala
3	M	39	MCD temporo-occipital basal	Occipital	Basal
4	M	47	DNET	Temporal	Middle temporal gyrus
5	F	40	Type II B cortical dysplsia	Prefrontal	DLPFC
6	F	35	Gliosis	Mesio-temporal	Amygdala
7	F	25	Type II cortical dysplasia	Temporal	Temporal pole
8	F	46	Type II cortical dysplasia	Temporal	Temporal pole
9	M	33	Type I cortical dysplasia	Frontal	Anterior cingulate cortex
10	M	28	Type I cortical dysplasia	Temporal	Hippocampus
11	F	25	N/A	Temporal	Entorhinal cortex

Table 1. List of patients included in this study

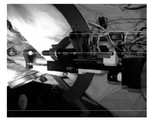

Figure 1. Acute microelectrode recording setup using clinical electrodes, stereotactic positioning, stimulation and recording instrumentation commonly used for functional mapping in deep brain stimulation procedures

Prior to the resective surgery, we are stereotactically inserting three microelectrodes, spaced 2mm apart, in a linear configuration, following a trajectory targeting SOZ. Standard clinical microelectrodes and equipment used in functional mapping for deep brain stimulation implantations was used. Bipolar electrical stimulation is applied in most cases between the two outer macro contacts of the electrodes, while recording the unit activity on the center microelectrode, located 3 mm deeper than the macro contacts. Constant current 0.5 to 1 mA biphasic pulses, 0.3 ms pulse width, frequency 1, 10, 30, 60 and 130 Hz were applied for 30 s using a clinical recording and stimulating system (Guideline LP+, FHC Inc, Bowdoin, ME). The interval before, between and after each electrical stimulation epoch was at least 30 seconds.

In order to remove the stimulation artifact, we used SALPA algorithm (Wagenaar and Potter, 2002). In addition, the noise introduced by connecting the stimulator to the macro contacts used for stimulation has been removed by using an adaptive noise cancellation filter (Widrow, 1975) using as reference the signal on one of the other microelectrode. This was possible as the stimulator noise on all channels is originating from a single source, therefore it is correlated across channels. Simultaneously sampled channels and built-in stimulation unit sharing the same clock as the recording unit resulted in a stimulation artifact without any pulse to pulse variability, therefore facilitating artifact removal (Hashimoto and Vitek, 2002). Spike sorting was performed using FIND toolbox (Meier et al., 2008).

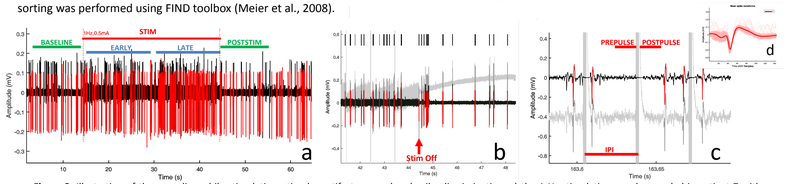

Figure 2. Illustration of the recording while stimulating, stimulus artifact removal and spike discrimination. a) the 1-Hz stimulation epoch recorded in patient 7 with discriminated neurons highlighted in red; b) a detail of the end of the stimulation epoch, showing the raw signal (gray) and the filtered signal. One has to note the noise band during stimulation that is significantly reduced. c) example of neurons recovered from the 30-Hz stimulation epoch. The blanking interval is 4.16 ms, accounting for 4.16% of the inter-pulse interval at 10 Hz and 25% at 60 Hz. d) mean spike waveform of the neuron presented in a), b) and c).

Firing rate histograms were calculated for the entire recording. Mean firing rates were calculated for the following intervals: a) pre-stimulation baseline – 10 s before each stimulation epoch; b) stimulation epoch; c) post-stimulation epoch – 10 s after each stimulation epoch; d) early stimulation – first 15 seconds of each stimulation; e) late stimulation – last 15 seconds of each stimulation. All firing rates were corrected for the duration of the blanking interval (4.16 ms in most cases).

Firing rate modulation indexes were calculated for a) assessing the effect of electrical stimulation, defined as the difference between mean firing rate during stimulation and the pre-stimulation baseline, divided by the sum of the two; b) assessing the time course of the stimulation, defined like the previous index, but using the early and late responses during each stimulation epoch.

$$MI_{STIM} = \frac{R_{STIM} - R_{BASELINE}}{R_{STIM} + R_{BASELINE}} \qquad MI_{BUILDUP} = \frac{R_{LATE} - R_{EARLY}}{R_{LATE} + R_{EARLY}} \qquad TLI = \frac{R_{POSTPULSE} - R_{PREPULSE}}{R_{POSTPULSE} + R_{PREPULSE}}$$

At the level of each stimulation pulse, we have calculated the time-locking index, defined as the difference between the activity in half of the inter-ulse interval (IPI) following each pulse and the activity in the half IPI preceding each stimulation pulse, divided by the sum of two.

Results

We have recorded to date 20 neurons in SOZ and adjacent areas. We were able to find several firing patterns in response to electrical stimulation: no-change (-0.25 < MI_{STIM}< 0.25), enhancement (MI_{STIM} > 0.25) or suppression (MI_{STIM} < -0.25), as shown in tables 2 and 3. The modulation is highly dependent on the stimulation frequency and pathology: 13 out of 14 neurons in SOZ exhibited suppression or enhancement at 30 Hz, compared to 4 out of 6 neurons outside SOZ. A buildup of the firing rate over the stimulation duration was observed in 12 (85.7%) of the SOZ neurons and 4 (66.6%) of the non-SOZ neurons at 30 Hz. Stimulation frequency above 30 Hz had a relative suppressive effect on the neuronal firing.

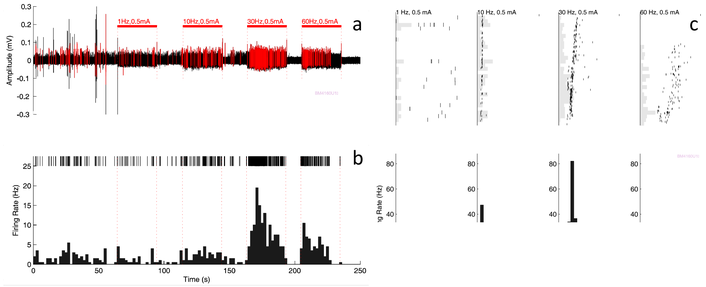

Figure 3. Illustration of a SOZ neuron highly modulated by the application of stimulation pulses, in patient #5 (prefrontal cortical dysplasia). The mean firing rate is little modified by the 1Hz stimulation (1.00 vs 1.70Hz), whereas at higher frequencies, it increases significantly to 2.57, 9.71 and 5.29 Hz for 10, 30 and 60 Hz, respectively. The higher firing rate is associated with increased time-locking of -0.25, 0.47, 0.93, 0.93 for the four stimulation frequencies.

The entrainment of the neurons by stimulation pulses, as reflected by the values of time-locking index varies significantly with the stimulation frequency. Individual pulses, applied at low repetition rate, are not able to evoke neuronal responses. However, when applied in a faster succession, initial pulses in a train seem to be able to pre-condition either individual neurons or the recurrent network connections, facilitating the response to subsequent pulses.

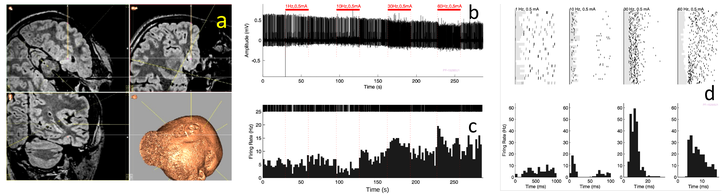

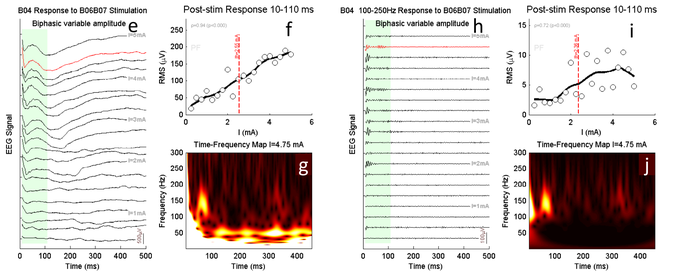

Figure 4. Correlation of single-unit firing pattern with EEG biomarkers of epileptogenicity during single-pulse electrical stimulation (SPES) in patient 10 (see Barborica et al 2013 for details) on SPES protocol). **(a)** Microelectrode trajectory shown on the MRI. The single unit was recorded from SOZ (Hc type I dysplasia). **(b)** Signal after artifact removal **(c)** Raster plot and firing rate histogram. **(d)** Peri-stimulus rasters and histograms for the inter-pulse interval. IPI histograms for 10 Hz and above exhibit a first peak around 10ms and a second one around 80 ms. **(e)** Unfiltered EEG response evoked by SPES in depth electrode's contact B03 (located in anterior Hippocampus, close to the microelectrode recording location) when stimulating on contact pair B05-B06 (located 3.5mm away). **(f)** Stimulus-response curve for pulses in the range 0.25 mA to 5 mA (3 ms, biphasic). **(g)** Time-frequency map of the responses, showing high-frequency oscillations (HFO) around 10 ms and 80 ms post-stimulation. **(h,i,j)** Similar to panel (e,f,g) but with the EEG signal filtered in the HFO frequency band (100-250Hz). The HFO at 10ms is now visible on both the EEG traces and the time-frequency map.

Considering that a network effect may be underlying timelocking facilitation, it may be possible that such neurons are involved in driving specific LFP/EEG responses hypothesized to be the result of pathological recurrent connectivity, like delayed responses (Valentin et al., 2002) and high-frequency oscillations (HFO, f > 80Hz) (van't Klooster et al, 2011). Such possible correlations are exemplified in figure 4 (lower panels), where delayed HFOs appear to have similar timing as single-unit activity (upper panels) recorded in the same cortical area of patient 10 (cortical dysplasia).

Single Unit Statistics

Stim epoch enhancement/suppression index

	All frequencies	1 Hz	10 Hz	30 Hz	60 Hz
All neurons	0.08±0.49, n=78	0.09±0.47, n=20	-0.03±0.39, n=20	0.20±0.55, n=20	0.07±0.55, n=18
SOZ	0.08±0.51, n=55	0.06±0.46, n=14	-0.09±0.36, n=14	0.20±0.59, n=14	0.15±0.61, n=13
non-SOZ	0.09±0.46, n=23	0.16±0.54, n=6	0.11±0.46, n=6	0.19±0.50, n=6	-0.14±0.33, n=5
n-way anova analysis					
Factor	p				
Patient	0.0107				
Pathology	0.1058				
Frequency	0.4707				

Timelocking index

	All frequencies	1 Hz	10 Hz	30 Hz	60 Hz
All neurons	0.16±0.42, n=78	-0.09±0.25, n=20	0.26±0.53, n=20	0.27±0.46, n=20	0.20±0.29, n=18
SOZ	0.22±0.48, n=55	-0.12±0.29, n=14	0.34±0.61, n=14	0.38±0.51, n=14	0.28±0.29, n=13
non-SOZ	0.01±0.11, n=23	-0.02±0.11, n=6	0.05±0.05, n=6	0.03±0.13, n=6	-0.02±0.15, n=5
n-way anova analysis					
Factor	p				
Patient	0.0001				
Pathology	0.0168				
Frequency	0.0024				

Stim epoch buildup index

	All frequencies	1 Hz	10 Hz	30 Hz	60 Hz
All neurons	-0.09±0.38, n=78	0.02±0.38, n=20	-0.07±0.29, n=20	-0.16±0.26, n=20	-0.18±0.54, n=18
SOZ	-0.14±0.40, n=55	-0.03±0.33, n=14	-0.13±0.31, n=14	-0.16±0.28, n=14	-0.25±0.62, n=13
non-SOZ	0.02±0.30, n=23	0.15±0.47, n=6	0.05±0.21, n=6	-0.15±0.22, n=6	0.01±0.18, n=5
n-way anova analysis					
Factor	p				
Patient	0.2023				
Pathology	0.1038				
Frequency	0.3016				

Table 1. N-way ANOVA analysis on single units data. The results show that only the patient selection had a significant effect (p<0.05) on the stimulation epoch enhancement/suppression index. All three factors (patients selection, pathology and stimulation frequency) had significant effect (p<0.05) on the timelocking index. In the case of stimulation epoch buildup index, none of the three factors showed a significant effect (p<0.05).

Pathology	Stim Epoch Pattern	Inter-Pulse Pattern	Frequency (Hz)																
			n	1 Baseline (Hz)	1 Stim Epoch (Hz)	1 Enhancement (+) / Suppression(-)	1 Time-locking index	n	10 Baseline (Hz)	10 Stim Epoch (Hz)	10 Enhancement (+) / Suppression(-)	10 Time-locking index	n	30 Baseline (Hz)	30 Stim Epoch (Hz)	30 Enhancement(+) / Suppression(-)	30 Time-locking index	n	60 Baseline (Hz)	60 Stim Epoch (Hz)	60 Enhancement(+) / Suppression(-)	60 Time-locking index
SOZ	**No-change**	**No-change**	3	4.6	4.5	0.7%	1.2%	1	13.6	11.9	-6.5%	-5.6%	0					0				
		Time-locked	1	6.3	5.0	-12.0%	-17.2%	0					1	6.6	7.4	5.6%	62.2%	3	5.1	4.9	-2.8%	23.0%
	Enhancement	**No-change**	2	0.2	4.5	66.7%	-2.4%	1	2.1	2.9	15.8%	-41.7%	3	1.2	5.0	61.5%	5.0%	3	2.8	9.1	74.9%	39.9%
		Time-locked	3	9.6	13.4	42.9%	-16.8%	4	2.9	5.3	35.1%	65.5%	6	3.8	9.3	54.7%	65.1%	3	1.5	6.5	65.1%	27.7%
	Suppression	**No-change**	5	8.8	4.0	-33.3%	-18.6%	3	11.6	4.9	-31.2%	11.4%	2	6.4	0.9	-75.8%	-46.2%	2	4.2	1.6	-59.0%	19.2%
		Time-locked	0					5	7.7	3.5	-35.8%	46.7%	2	8.7	3.5	-43.0%	74.9%	2	5.4	2.0	-46.8%	27.0%
	Buildup	**No-change**	7	6.3	5.0	8.1%	-4.7%	2	15.5	6.1	-36.8%	18.2%	5	3.2	3.3	6.6%	-15.5%	4	2.2	3.0	17.0%	31.2%
		Time-locked	0					5	4.7	2.9	-6.0%	47.2%	7	4.3	6.4	29.5%	72.9%	7	3.4	4.6	14.0%	30.6%
Normal	**No-change**	**No-change**	1	1.3	1.2	-5.0%	-2.5%	3	6.3	5.5	-5.5%	2.7%	0					0				
		Time-locked	0					0					2	7.4	8.1	4.7%	-5.2%	2	7.3	7.6	-0.1%	-7.5%
	Enhancement	**No-change**	4	3.6	8.1	41.8%	-4.4%	2	0.6	3.7	61.6%	5.8%	3	1.1	3.7	54.1%	13.9%	1	2.0	3.2	22.4%	24.0%
		Time-locked	0					0					0					0				
	Suppression	**No-change**	1	1.6	0.3	-66.0%	8.0%	1	5.1	2.1	-41.1%	8.2%	1	3.4	0.9	-57.6%	-14.0%	2	2.8	0.9	-45.8%	-10.6%
		Time-locked	0					0					0					0				
	Buildup	**No-change**	5	2.2	5.1	16.0%	-4.1%	3	3.2	3.4	8.1%	7.1%	3	1.5	1.5	16.8%	6.6%	2	3.1	2.1	-18.5%	5.0%
		Time-locked	0					0					1	7.6	8.1	3.3%	-5.5%	0				

Table 2. Single-unit classification based on pathology, stimulation epoch pattern and inter-pulse pattern.

Conclusions

- Time-locking is associated with pathological cortex.
- Only frequencies of 10 Hz and above result in significant timelocking.
- Higher frequencies (30 Hz) have an excitatory effect, particularly in pathological tissue.

This study highlights the firing rate properties of single units in epileptogenic cortex. The results have implications in understanding the basic mechanisms underlying epileptogenic networks and in modulating the neuronal activity through electrical stimulation.

Acknowledgments

We would like to thank Mihai Malîia, Alin Rasina, Bogdan Balanescu and Irina Popa for their contribution to this study.

Grant support: Romanian government UEFISCDI research grant PN-II-ID-PCE-2011-3-0240.

References

1. Barborica A, Donos C, Ciurea J, Rasina A, Balanescu B, Mindruta I. Stimulus Amplitude Effect In Time And Frequency On Responses To Single Pulse Electrical Stimulation In Stereoelectroencephalographic Studies, The 30th International Epilepsy Congress,Montreal, Canada, 23–27 June, 2013, Epilepsia, 54(S3):267–268, 2013.
2. David O, Woźniak A, Minotti L, Kahane P. Preictal short-term plasticity induced by intracerebral 1 Hz stimulation. Neuroimage. 2008 Feb 15;39(4):1633-46.
3. Hashimoto T, Elder CM, Vitek JL. A template subtraction method for stimulus artifact removal in high-frequency deep brain stimulation. J Neurosci Methods. 2002 Jan 30;113(2):181-6.
4. Meier R, Egert U, Aertsen A, Nawrot MP. FIND - a unified Framework for neural data analysis; Neural Netw. 2008 Oct; 21 (8): 1085-93
5. Valentin A, Anderson M, Alarcon G, Seoane JJ, Selway R, Binnie CD, Polkey CE. Responses to single pulse electrical stimulation identify epileptogenesis in the human brain in vivo. Brain 2002;125:1709–1718.
6. van 't Klooster MA, Zijlmans M, Leijten FS, Ferrier CH, van Putten MJ, Huiskamp GJ. Time-frequency analysis of single pulse electrical stimulation to assist delineation of epileptogenic cortex. Brain 2011;134:2855-2866.
7. Wagenaar DA, Potter SM. Real-time multi-channel stimulus artifact suppression by local curve fitting. J Neurosci Methods. 2002 Oct 30;120(2):113-20.
8. Widrow B, Glover JR, McCool JM, Kaunitz J et al. Adaptive noise cancelling: Principles and Applications. Proc. IEEE, 1975;46(8):1151-1162